Proceedings of the XVIII ECSMGE 2024
GEOTECHNICAL ENGINEERING CHALLENGES
TO MEET CURRENT AND EMERGING NEEDS OF SOCIETY

ISBN 978-1-032-54816-6
DOI 10.1201/9781003431749-33

ECSMGE 24
XVIII EUROPEAN CONFERENCE
ON SOIL MECHANICS AND
GEOTECHNICAL ENGINEERING

1-D intrinsic compression curves for settlement analysis of soft clays

Courbes de compression monodimensionnelles intrinsèques pour l'analyse de tassements d'argiles mous

C. Athanasiu
Multiconsult Norge AS, Oslo, Norway

A.B. Tsegaye*
Norwegian Geotechnical Institute, formerly Multiconsult, Trondheim, Norway

E.R. Sørlie
Multiconsult Norge AS, Oslo, Norway

K.E.L. Johnsen
Løvlien Georåd AS, formerly Multiconsult ASA

**anteneh.biru.tsegaye@ngi.no*

ABSTRACT: Settlements in soils occur due to changes in effective stress (instant settlements) and creep in time during and after application of the effective stress changes (delayed settlements). In soft clays, the delayed settlement can be significant and must be accounted for. This paper presents a settlement analysis method that accounts for both instant and delayed components. Relations between accumulated creep strain, apparent age of the soil layer and the pre-consolidation stress due to creep are established as 1-D Intrinsic Compression Curves (1-D ICC). The paper describes the parameters used with the 1-D ICC method and how they can be determined from the constant rate of strain (CRS) oedometer tests including a creep phase. The construction and the use of 1-D ICC method to model the settlement development with time during and after consolidation process are also presented.

RÉSUMÉ: Les tassements du sol se produisent en raison de changements dans la contrainte effective (tassements instantanées) et de fluage, en temps, pendant et après l'application des changements de contrainte effective (tassements retardés). Dans les argiles molles, les tassements retardés peuvent être importants et doivent être pris en compte. L'article présente une méthode d'analyse des tassements qui prend en compte à la fois les composantes instantanées et retardés. Les relations entre la déformation de fluage accumulée, l'âge apparent de la couche de sol et la contrainte apparente de pré-consolidation due au fluage sont établies sous forme de Courbes de Compression Intrinsèques en problème monodimensionnel, CCI 1-D. L'article décrit les paramètres utilisés avec la méthode CCI 1-D et comment la méthode peuvent être utilisée pour modéliser le développement des tassements dans le temps.

Keywords: Oedometer tests; instant and delayed strains; embankment settlements.

1 INTRODUCTION

Bjerrum (1967) postulated the concept of instant, $\Delta\varepsilon_i$, and delayed, $\Delta\varepsilon_d$, compression strain due an increase in effective vertical stress, $\Delta\sigma'_v$, and due to creep in a period, Δt, under constant effective stress, respectively, Figure 1.

Based on results from oedometer tests conducted with different periods of time to creep under constant effective stress after consolidation, Bjerrum postulated that lines with equal creep rate, isotaches, are parallel with the Instant 1-D compression line, Figure 2.

The isotache concept and the insight into the creep behaviour of soils have been accumulated in time over many decennia (Den Haan, 2007).

The aim of the paper is to present a simplified method for calculating settlements of soft clays accounting for instant and delayed (creep) compression strains.

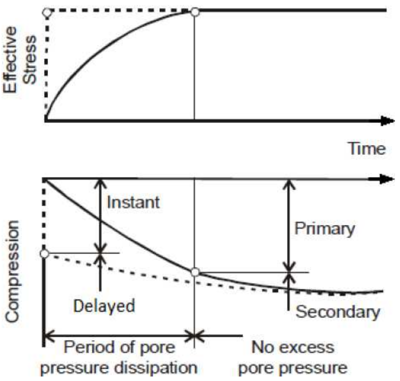

Figure 1. Instant and delayed compression (Bjerrum, 1967).

The method is based on a simplified formulation of tangent creep resistance as a function of apparent age and on an intrinsic compression curve of accumulated delayed strain, ε_c, vs. age of the clay deposit, t_a.

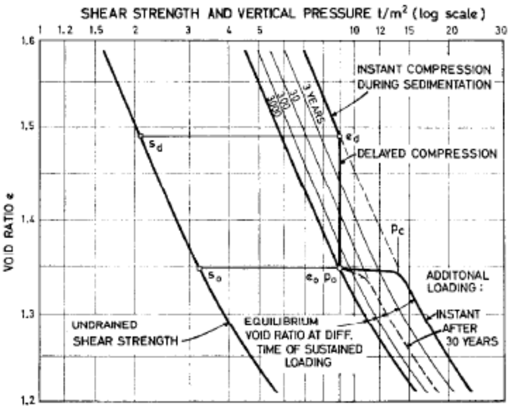

Figure 2. e-log σ'ᵥ diagram showing isotaches (Bjerrum, 1967).

2 INSTANT AND DELAYED COMPRESSION STRAINS

The calculation of compression strains (settlements) due to an increase in effective stress from σ'_1 to $\sigma'_2 = \sigma'_1 + \Delta\sigma'$ in a period of time from t_1 to $t_2 = t_1 + \Delta t$ can be performed separately for instant and creep part, if the stress and time increments, $\Delta\sigma'$ and Δt are small enough to neglect the parameter variation with stress and time.

The delayed (creep) strain increment due to a time interval from t_1 to t_2 can be expressed as:

$$\Delta\varepsilon_{del} = \mu^* \cdot ln\left(\frac{t_2}{t_1}\right) = \frac{1}{r_s} \cdot ln\left(\frac{t_2}{t_1}\right) = \frac{C_\alpha}{(1+e_o)} log\left(\frac{t_2}{t_1}\right) \quad (1)$$

where e_o is the void ratio, and μ^*, r_s, and C_α are tangent creep parameters (for a time interval, Δt_a, from $t_1 = t_a$ to $t_2 = t_a + \Delta t_a$).

The increment of instant strain due to an increment of effective stress from σ'_1 to σ'_2 is calculated as: for $\sigma'_1 < p'_c < \sigma'_2$:

$$\Delta\varepsilon_{inst} = \kappa'^* \cdot ln\left(\frac{p'_c}{\sigma'_1}\right) + \lambda^* \cdot ln\left(\frac{\sigma'_2}{p'_c}\right) \quad (2)$$

The parameters $\kappa'^* = \frac{C'_s}{(1+e_0)\ln 10} = \frac{1}{m'_{OC}}$ refer to instant (without creep) compression within the over consolidation (OC) stress range in contrast to $\kappa^* = \frac{C_s}{(1+e_0)\ln 10} = \frac{1}{m_{OC}}$ which refer to total, instant including creep compression (as measured in oedometer tests) in the same, OC range.

By equating creep strain with plastic strain in normal consolidation range, (Leroueil et al., 1985), found that the ratio of the effective stresses, σ'_1 and σ'_2, at the same strain, measured in two oedometer tests with the same soil and initial state performed with two different strain rates, $\dot{\varepsilon}_1$ *and* $\dot{\varepsilon}_2$, are related by:

$$\frac{\sigma'_1}{\sigma'_2} = \left(\frac{\dot{\varepsilon}_2}{\dot{\varepsilon}_1}\right)^B, \; B = \frac{C_\alpha}{C_c} = \frac{\mu^*}{\lambda^*} = \frac{m_{NC}}{r_s} \cdot \quad (3)$$

Consequently, in the NC range, the rate parameter, B, is related to C_α and C_c as given in Eq. (3), and is found to depend on the type of clay (Mesri and Godlewski, 1977; Leroueil et al., 1985). The Eq. (3) is based on Janbu's definition of constrained modulus in NC range (Janbu, 1963), where σ'_r is the reference stress.

Following the Eq. (3), a relation can be obtained between creep and compression parameters in NC range:

$$\mu^*_{NC} = \frac{B}{M/\sigma'} = \frac{B}{m_{NC}} \quad (4)$$

in which M is the compression tangent constrained modulus and σ' is the applied effective stress in NC range.

Laboratory tests show that the isotaches corresponding to a constant ratio t_{ai}/t_{ai-1} are not equidistant but are narrower as the apparent age increases and, consequently, that the creep rate decays more than linear with log of time, Figure 3.

Figure 3a presents the results from special compression tests with four 125 mm long, sub-elements connected in series by (Mesri and Feng, 1986 and Mesri et al., 1995). Leroueil et al. (1986) and Leroueil and Marques (1996) reinterpreted the results to define the compression curves of each sub-element subjected to consolidation under a pressure increment from 97 to 138 kPa, followed by creep phase at constant stress of 138 kPa. Also drawn on the figure is a fictitious isotaches assuming B= 0.03 for St-Hilaire clay. The set of isotaches coincides very well with the observed behaviour. The blue points in Figure 3b are constructed as follows. The void ratio at the intersection between an isotache and the vertical line corresponding to constant stress of 138 kPa in Figure 3a is plotted against the strain rate of this isotache (the lower horizontal axis). The plot e vs. strain rate shows that the isotaches are not equidistant (Δe from 10^{-8} to 10^{-9} min^{-1} is less than Δe from 10^{-5} to 10^{-6} min^{-1}).

In our opinion the compression curves of the four sub-elements in Figure 3 include both instant and delayed compression strains (Hypothesis B). The monitored strain rates match the set of isotaches and prove that the clay behaviour is strain rate dependent during primary consolidation.

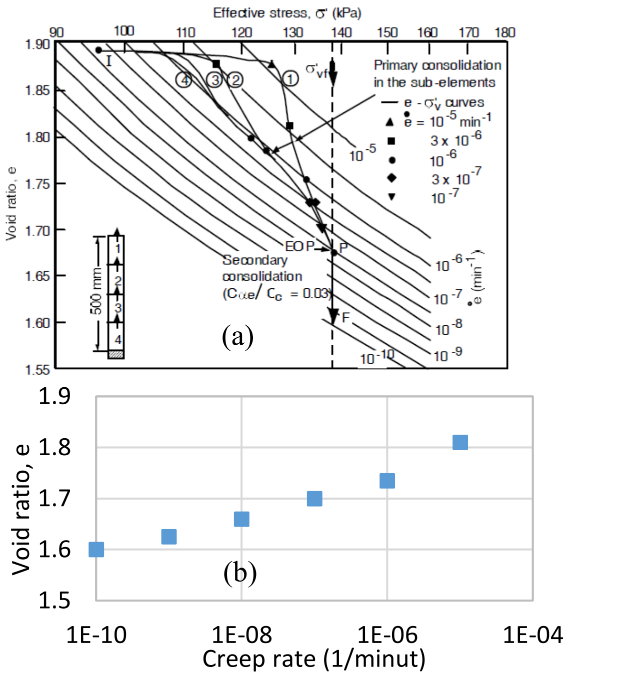

Figure 3. a) Consolidation of Saint-Hilaire clay; from Mesri et al. (1995); from Leroueil (2006) b) Void ratio versus creep rate from the data in figure (a).

Further arguments for hypothesis B may be found in Degago et al. (2011).

The results shown in Figure 3a are used to obtain a picture of distance between two consecutive isotaches in log scale as a function of creep rate. As the isotaches represent lines of equal creep rate and, at the same time, lines of equal creep time, the relation between creep rate and time is found from the definition of creep rate:

$$\dot{\varepsilon}_c = \frac{\mu^*}{t} \tag{5}$$

If creep parameter, μ^*, is independent on time, the isotaches are equidistant. The blue point curve, constructed as void ratio distance between two consecutive log cycle creep rates (10^{-5} 1/min, 10^{-6} 1/min, and so on) at stress 138 kPa, shows, however, that the isotaches are not equidistant, indicating a non-linear creep parameter.

The non-linearity of creep parameter has been discussed by many researchers, e.g., (Watabe et al., 2012, Karim and Lo, 2020, Yuan et al., 2015), (Vergote et al., 2021). Based on several CRS oedometer tests including creep phases under constant stress, the following expression is proposed for creep parameter as a function of time:

$$\mu^* = \frac{\mu^*_{NC}}{\left[1+\alpha \cdot ln\left(\frac{t}{t_{inst}}\right)\right]} \tag{6}$$

where α is empirical factor determined experimentally. t_{inst} is the time corresponding to virgin (instant) compression line along which only instant strains are developed as a function of applied effective stress (no creep strains.) A value of 1 second is assumed for t_{inst}.

Using Eqs. (5) and (6) we obtain the differential equation for the accumulated creep strain rate at the time t:

$$d\varepsilon_c = \mu^* \cdot \frac{dt}{t} = \frac{dx}{r_{sNC} \cdot x \cdot [1+\alpha \cdot ln(x)]} \tag{7}$$

with $x = t/t_{inst}$. The differential equation (7) is integrated to obtain the accumulated creep strain at age, t_a, under constant effective stress, p'_0:

$$\varepsilon_c = \frac{1}{D} ln \left[1 + \alpha \cdot ln\left(\frac{t_a}{t_{inst}}\right)\right] \tag{8}$$

where $D = r_{sNC} \cdot \alpha$

From Eq. (8) we can obtain a relation between the apparent age, t_a, and the accumulated creep strain, ε_c, as:

$$t_a = t_{inst} \cdot exp\left\{\frac{1}{\alpha} \cdot [exp(D \cdot \varepsilon_c) - 1]\right\} \tag{9}$$

If accumulated creep strain is equated to plastic strain, the intrinsic relation between over-consolidation ratio and age is obtained as:

$$\frac{p'_c}{p'_o} = \left[1 + \alpha \cdot ln\left(\frac{t_a}{t_{inst}}\right)\right]^A \tag{10}$$

with $A = \frac{1}{D \cdot (\lambda^* - \kappa'^*)}$.

The pre-consolidation pressure, p'_c, is defined by the intersection between unloading-reloading line (with slope κ'^*) from p'_0, ε_0 and instant compression line (slope λ^*) in contrast to the apparent, oedometer pre-consolidation stress, p'_{ca}, defined at the intersection between unloading-reloading line (slope

κ^*, without delayed strains) from p'_0, ε_0 and oedometer isotach (slope λ^*), as seen in Figure 4.

To verify the validity of the proposed formulation for creep parameter, an attempt is made to model experimental results of normalized pre-consolidation (p'_{ca}/p'_{c0}) where p'_{c0} is the apparent pre-consolidation stress at a strain rate of 10^{-7} 1/s, as a function of creep rate, Figure 5. The blue line depicts the relationship predicted based on Eq.(6). As seen from Figure 5, the agreement of prediction to measurements is encouraging. Similar good agreement is shown in Figure 6 for Osaka Bay clays.

Experimental results show also that r_s is low when creep is measured at effective stress, $\sigma' \geq p'_{ca}$, and r_s increases gradually as the ratio σ'/p'_{ca} decreases, (e.g., Christensen, 1985). This is since the age of the clay and, consequently, r_s, increases as σ'/p'_{ca} decreases.

Using the proposed formulation of creep parameter, Eq.(6), and combining Eqs.(8)-(10), the relation between μ* (or r_s) and σ'/p'_{ca} is obtained as follows:

$$\mu^* = \frac{1}{r_s} = \mu^*_{NC} \cdot \left(\frac{\sigma'}{p'_{ca}}\right)^{1/A} \qquad (11)$$

The results of creep oedometer tests on Bangkok clay, showing measured r_s vs. σ'/p'_{ca} and the relation predicted by Eq. (11) are shown in Figure 7.

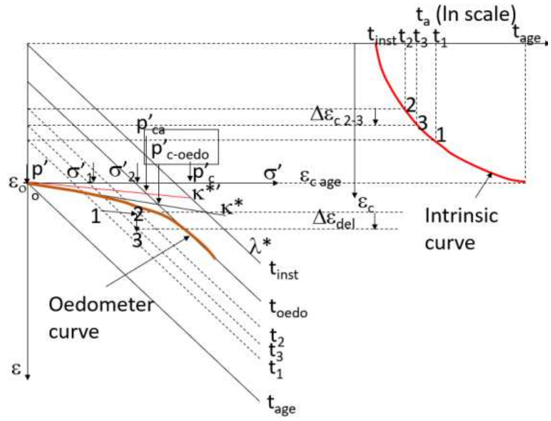

Figure 4. Intrinsic creep strain curve: ε_c vs. ln (t_a).

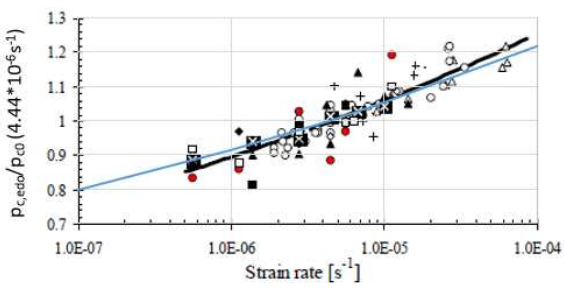

Figure 5. Normalized pre-consolidation vs. strain rate at a strain of 10% for finish clays, from (Leroueil et al., 1985). Blue line prediction uses Eq.(6) and α=0.005, λ*=0.35, k*'=0.002 and r_{sNC}=44.

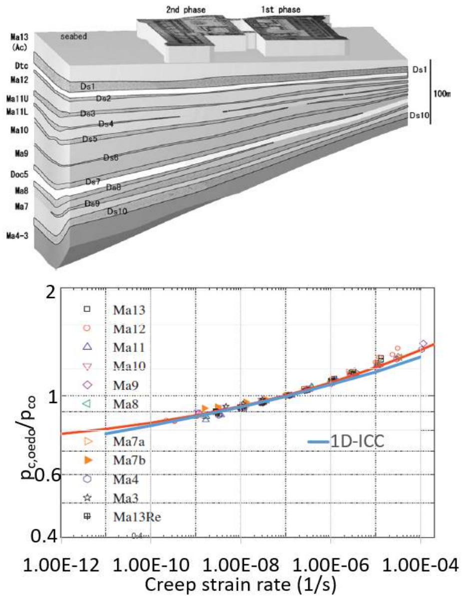

Figure 6. a. Stratigraphy model of Kansay International Airport; b. p'_{ca}/p'_{c0}-log $\dot{\varepsilon}_c$ relationship for clays at Osaka Bay (red curve – proposed trend line, (Watabe et al., 2012), blue curve predicted by Eq. (6)). ($\alpha = 0.1$; $\lambda^* = 0.3$; $\kappa^{*\prime} = 0.002$; $r_{sNC} = 47$).

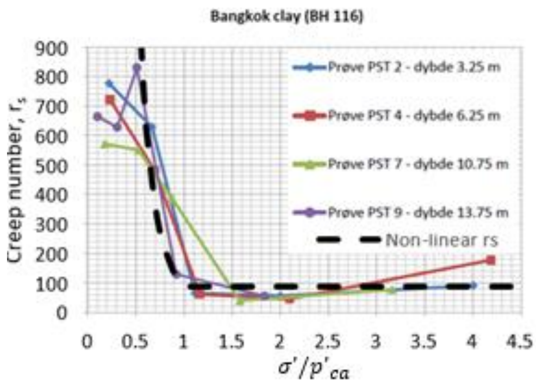

Figure 7. Variation of r_s with σ'/p'_{ca} (Athanasiu, 2012).

3 SOFT CLAY BEHAVIOR UNDER LOADING AND INTRINSIC CURVES

Experimental results reveal that creep rate decreases with time (Figure 3 and Figure 7) and that stress-strain curves obtained in oedometer tests depend on the rate of strain at which the test is performed (Figure 5 and Figure 6)

The accumulated creep strain during consolidation in geological time can be described by an intrinsic relation (1-D Intrinsic Compression Curve) between accumulated creep strain and apparent age of the deposit, ε_c vs. t_a, Eq. (8) as shown in Figure 4.

The 1-D ICC is the “fingerprint” of the creep geological history of the clay deposit.

The strain changes due to changes in stress and time can be calculated using the frame of 1-D ICC as follows.

Let the point 1 in Figure 4 describe the stress-strain-age (σ'_1, ε_{c1}, p'_{c1} and t_1) conditions before a new load change is applied. If the effective stress is increased from σ'_1 to σ'_2, the apparent age will be changed from t_1 to $t_2 < t_1$ (the clay becomes "younger" and with a lower accumulated creep strain). The increment of instant strain, $\Delta\varepsilon_{inst}$, is calculated using Eq.(2).

The preconsolidation stress remains unchanged, $p'_{c2} = p'_{c1}$ if $\sigma'_2 < p'_{c1}$ but must be updated, $p'_{c2} = \sigma'_2$ if $\sigma'_2 > p'_{c1}$.

The accumulated creep strain, is then calculated as plastic strain:

$$\varepsilon_{c,2} = (\lambda^* - \kappa'^*) \cdot \frac{p'_{c,2}}{\sigma'_2} \tag{12}$$

and the apparent age t_2 is calculated using Eq.(9). Let the time required by consolidation process to increase effective stress from σ'_1 to σ'_2 be Δt . The change in delayed strain due to Δt is equal to the increase in intrinsic accumulated strain from ε_{c2} to ε_{c3} where ε_{c3} corresponds to the apparent age in point 3 ($t_3 = t_2 + \Delta t$) and can be calculated using Eq.(8). The change in delayed strain is then calculated as:

$$\Delta\varepsilon_{del} = \varepsilon_{c,3} - \varepsilon_{c,2} \tag{13}$$

The pre-consolidation stress at point 3 must now be updated due to age changing to t_3 using Eq.(9) to obtain p'_{c3}/σ'_3, ($\sigma'_3 = \sigma'_2$) as a function of t_3.

The procedure described above can be repeated for all steps of a consolidation process, where in each step the stress-strain-age state of point 1 is updated from the stage at point 3 in previous step.

4 CALIBRATION OF PARAMETERS USING THE CREEP PART OF OEDOMETER TEST

During the creep part of the oedometer test the effective stress is, theoretically, kept constant. Care must be taken to align the measured time, t_m, with the apparent age time, t_a: at the start of the creep test, t_a is equal to t_{oedo}, Figure 8.

The calibration requires two sets of simple iterations, one for compression indices, (λ^* or m_{NC}, κ^* and $\kappa^{*\prime}$) and one for creep parameters (B or r_{sNC} and α). The accuracy of the geological age of a clay deposit depends on how well the geological history of the deposit is known. In addition, it is assumed that pre-consolidation pressure is induced exclusively by creep, i.e., the clay is NC, aged clay.

The comparison between measured and computed accumulated strains are shown in Figure 9.

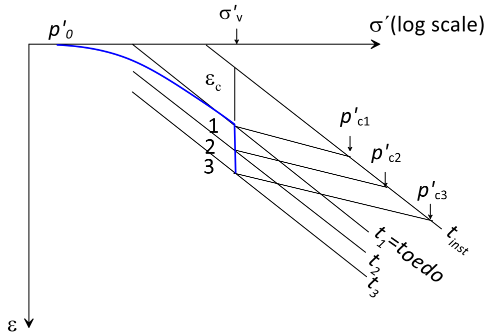

Figure 8. Creep test part starts on t_{oedo} line.

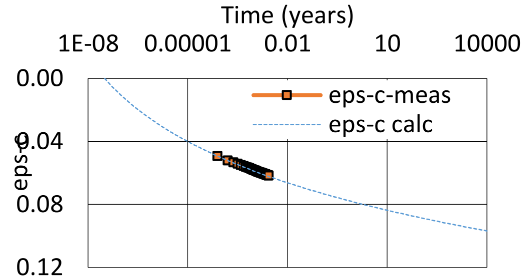

Figure 9. Comparison of measured and computed creep strains during creep part of the test.

5 BACK-CALCULATION OF OEDOMETER TEST

Next the calibration of 1-D ICC method is illsustrated using incremental oedometer loading (IL) test results of samples taken from the well-known Väsby test fill, Sweden.

The Väsby test fill (Chang, 1981), consists soft sediments of glacial and post-glacial origin.

Figure 10 presents the results of incremental loading (IL) oedometer test on sample taken with 200 mm Laval sampler from 4.2 m depth (Leroueil et al., 1985, Degago and Grimstad, 2016).

The consolidation and creep settlement parameters resulted from matching the oedometer curve with the back-calculated curve in Figure 10, are presented in Table 1.

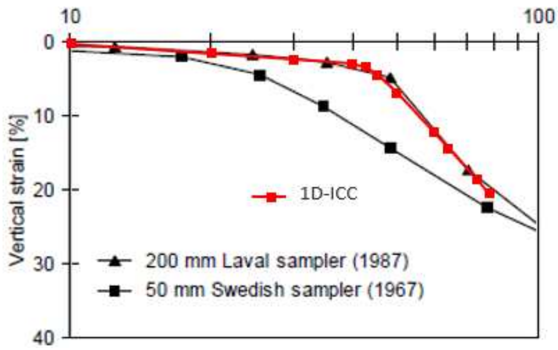

Figure 10. Calibration of incremental oedometer test results on samples taken at 4.2 m from Väsby field depth using two different samplers, data from (Leroueil and Kabbaj, 1987).

Table 1. Calibrated parameters.

Parameter	Units	Value
κ^*	-	0.1
λ^*	-	0.3
κ'^*	-	0.02
B	-	0.06
α	-	0.06
t_{age}	years	1000
p'_{ca}	kPa	44.9
$p'_{c\text{-}oedo}$	kPa	50
p'_0	kPa	30

6 CONCLUSIONS

A time resistance formulation is proposed to describe the variation of creep parameter, μ^*, with apparent age of a clay sediment.

Experimental results are compared to those predicted by the proposed formulation and the comparison shows fair good agreement.

The paper defines an intrinsic compression curve of accumulated creep strain of a clay layer effectively supporting the overburden pressure throughout the age of the deposit. This is used as a framework to calculate instant and delayed strains caused by steps of effective stress and time increments.

ACKNOWLEDGEMENTS

The authors are indebted to their colleagues, particularly to Anders Bye and Joar Spencer Gloppestad for fruitfull discussions regarding the consequences of delayed strains on settlements of offshore structures.

The contribution from workshops organized at Norwegian University of Science and Technology, NTNU, on creep settlements are also gratefully aknowledged.

REFERENCES

Athanasiu, C. (2012). Experience on calculating consolidation and creep deformations. Advanced models with applications to embankments. PLAXIS Course, NTNU, Trondheim.

Bjerrum, L. (1967). Engineering geology of Norwegian Normally-consolidated marine clays as related to settlements of buildings. *Géotechnique* 17 (2): 83-118.

Chang, C. E. H. (1981). Long term consolidation beneath the test fills at Vasby, Sweden. SGI Repport No 13.

Christensen, S. (1985). Creep tests in oedometer, Eberg clay, SINTEF Division of Geotechnical Engineering.

Degago, S. and Grimstad, G. (2016). Evaluation of soil parameters for creep calculations of field cases. *Proc. of the 17th Nordic Geotechnical Meeting*. Reykjavik, Island.

Degago, S. A., Grimstad, G., Jostad, H. P., Nordal, S. and Olsson, M. (2011). Use and misuse of the isotache concept with respect to creep hypotheses A and B. *Géotechnique* 61(10): 897-908.DOI: 0.1680/geot.9.P.112.

Den Haan, E. (2007). A history of the development of Isotache models. DOI:10.13140/ RG.2.2.32972.13441.

Janbu, N. (1963). Soil compressibility as determined by oedometer and triaxial tests. *Proc. 3rd Eur. Conf. Soil Mech*., Weisbaden.

Karim, M. R. and Lo, S. C. R. (2020). Non-linearity of creep coefficient. *Geotechnical Research* 7(2):90–95.DOI: https://doi.org/10.1680/jgere.19.00018.

Leroueil, S. (2006). The isotache approach. Where are we 50 years after its development by Professor Suklje? Suklje Memorial Lecture.

Leroueil, S. and Kabbaj, M. (1987). Discussion of 'Settlement analysis of embankments on soft clays' by Mesri & Choi. *ASCE* 113(9): 1067-1070.

Leroueil, S., Kabbaj, M., Tavenas, F. and Bouchard, R. (1985). Stress–strain–strain rate relation for the compressibility of sensitive natural clays. *Géotechnique*35(2):159-180. DOI:10.1680/geot. 1985.35.2.159.

Leroueil, S. and Marques, M. E. S. (1996). Importance of Strain Rate and Temperature Effects in Geotechnical Engineering.

Mesri, G. and Feng, T. W. (1986). Stress-strain-strain rate relation for the compressibility of sensitive natural clays. Discussion. *Géotechnique* 36(2): 283–290.

Mesri, G., Feng, T. W. and Shahien, M. (1995). Compressibility parameters during primary consolidation. *Proceedings, International Symposium on Compression and Consolidation of Clayey Soils*, Hiroshima, Japan.

Mesri, G. and Godlewski, P. M. (1977). Time and stress-compressibility interrelationship. *ASCE J Geotech Eng Div* 103(5): 417-430.

Vergote, T. A., Leung, C. F. and Chian, S. C. (2021). Elastoviscoplastic modelling with distorted isotaches and swelling for constant strain rate and incremental loading. *International Journal for Numerical and Analytical Methods in Geomechanics* 45(13).DOI: 10.1002/nag.3248.

Watabe, Y., Udaka, K., Nakatani, Y. and Leroueil, S. (2012). Long-term consolidation behavior interpreted with isotache concept for worldwide clays. *Soils and Foundations* 52(3): 449-464.DOI: https://doi.org/10.1016/j.sandf.2012.05.005.

Yuan, Y., Whittle, A. J. and Nash, D. F. T. (2015). Model for Predicting and Controlling Creep Settlements with Surcharge Loading. *Deformations Characteristics of Geomaterials*: 931–938.DOI: doi:10.3233/978-1-61499-601-9-931.